Supporting Information

Highly Sensitive and Reusable Membraneless Field Effect Transistor (FET)-type Tungsten Diselenide (WSe_2) Biosensor

Hae Won Lee[1+], Dong-Ho Kang[2+], Jeong Ho Cho[3], Sungjoo Lee[2,3], Dong-Hwan Jun[4,], and Jin-Hong Park[1,2,3,*]*

[1] School of Semiconductor and Display Engineering, Sungkyunkwan University, Suwon 16419, Korea

[2] School of Electronic and Electrical Engineering, Sungkyunkwan University, Suwon 16419, Korea

[3] SKKU Advanced Institute of Nano Technology (SAINT), Sungkyunkwan University, Suwon 16419, Korea

[4] Korea Advanced Nano Fab Center (KANC), Suwon 16229, Korea

*Corresponding Author : jhpark9@skku.edu (Prof. J.-H. Park), donghwan.jun@kanc.re.kr (Dr. D.-H. Jun)

Thickness of WSe_2 flake as analyzed by AFM

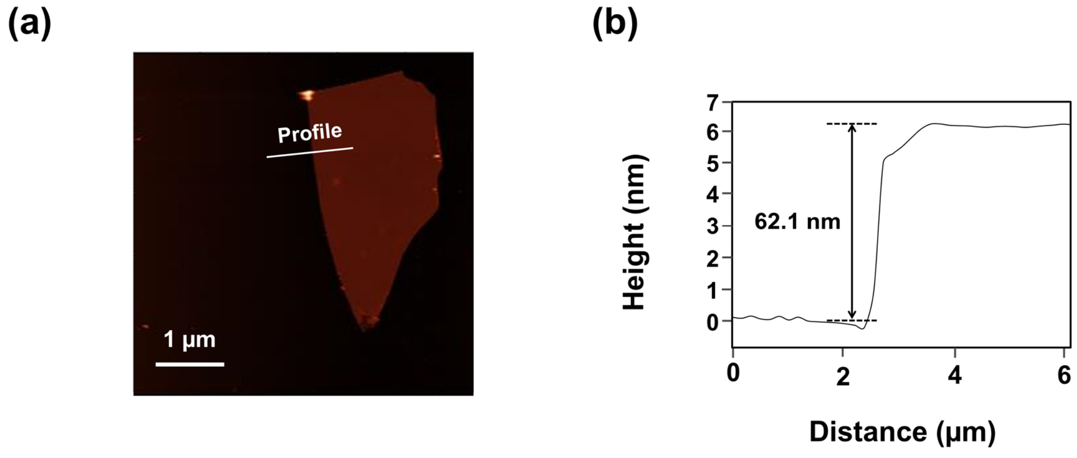

Figure S1. (a) AFM analysis on WSe_2 flake. (b) Extracted profile from the AFM analysis, which exhibits the thickness of 62. 1 nm.

I_D-V_G characteristics after rinsing process and during 6 cycles with different glucose concentrations

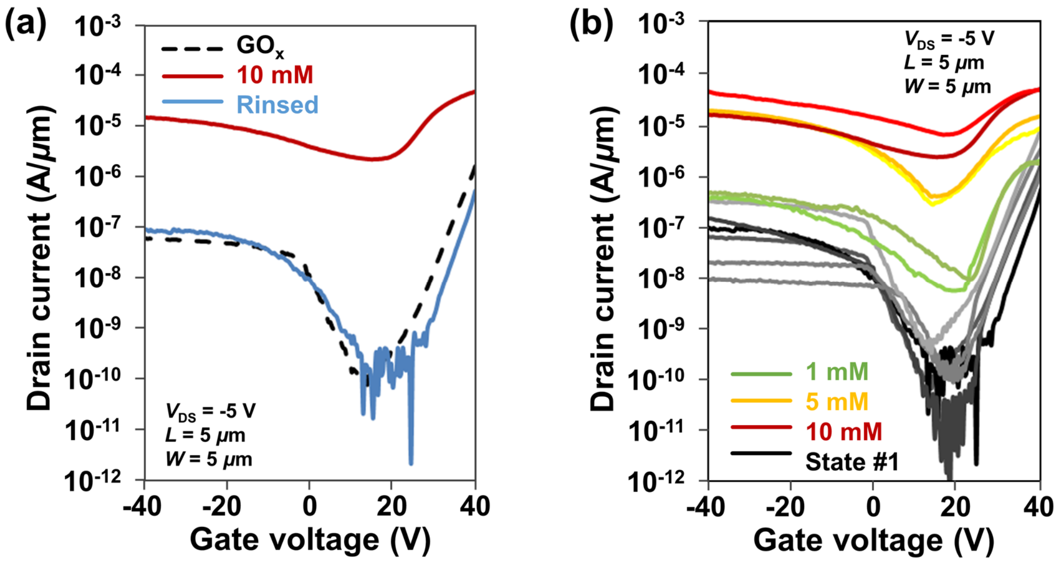

Figure S2. a) I_D-V_G characteristics of the WSe_2 BioFET in GOx-immobilized state, glucose-sensed state (10 mM), and rinsed state. (b) I_D-V_G characteristics of the WSe_2 BioFETs in the repeated rinsing and applying glucose steps with different concentrations (1, 5, 10 mM)

Figure S2a shows the I_D–V_G characteristics of the WSe_2 BioFET in the GO_x-immobilized state (black dotted line), glucose-sensed state (red line), and rinsed state (blue line). The current values in the GO_x-immobilized state (state #1) and rinsed state were almost the same, indicating that glucose was fully removed through the rinsing step. It also appears that the created surface defects hold the chemical linker APTES well even after rinsing glucose, thereby returning the device to state #1.With confirmation of thorough removal of glucose, we repeated the cycles of rinsing and applying glucose. The whole I_D-V_G curves of the WSe_2 BioFETs in different concentrations (1, 5, 10 mM) are presented in Figure S2b, where the sensitivity values were extracted and shown in Figure 4c.

Performance comparison with other biosensors.

Type of biosensor	Channel Materials	Detection molecules	Detection range	Sensitivity	Reusability	Reference
Electrochemical (CV and CA)	$Bi_2O_2CO_3$ nanoplates	Cholesterol	0.05 - 7.4 mM	139.5 μAmM^{-1}cm^{-2}	No mention	[S1]
Electrochemical (CV and CA)	ZnO nanotubes	Cholesterol	1 μM - 13 mM	79.4 μAmM^{-1}cm^{-2}	No mention	[S2]
Electrochemical (CV and CA)	Au-PAni	Glucose	1 μM - 20 mM	29.27 ± 0.73 μAmM^{-1}cm^{-2}	No mention	[S3]
Fluorescent	CdSe/ZnS	Glucose	0.045 - 10 mM	Fluorescence intensity 48000	No mention	[S4]
Fluorescent	MoS_2	DNA	0.5 - 130 nM	Fluorescence intensity 25 - 250	No mention	[S5]
FET	rGO/C-PPy nanotubes	Glucose	1 nm - 100 mM	0.45 A/A	No mention	[S6]
FET	Si nanowires	PSA	0.023 - 500 ng/mL	70 mV/pH	No mention	[S7]
FET	In_2O_3 nanoribbons	Glucose	0.1 μM - 1 mM	3 A/A	No mention	[S8]
FET	MoS_2	pH	pH 3 - 9	713 A/A	No mention	[S9]
FET	MoS_2	Doxorubicin	0.1 nM - 50 μM	1757.1 A/A	Reusable	[S10]
FET	WSe_2	Glucose	1 - 10 mM	2.87×10^5 A/A	Reusable	This work

Table S1. The performance comparison table in terms of biosensor type, channel material, detection molecule, sensitivity, and reusability.

[S1] Umar, A.; Ahmad, R.; Kumar, R.; Ibrahim, A. A.; Baskoutas, S. $Bi_2O_2CO_3$ nanoplates: Fabrication and characterization of highly sensitive and selective cholesterol biosensor. *J. Alloys Compd.* **2016**, *683*, 433-438.

[S2] Ahmad, R.; Tripathy, N.; Kim, S. H.; Umar, A.; Al-Hajry, A.; Hahn, Y. –B. High performance cholesterol sensor based on ZnO nanotubes grown on Si/Ag electrodes. Electrochem. Commun. **2014**, *38*, 4-7.

[S3] Chowdhury, A. D.; Gangopadhyay, R.; De, A. Highly sensitive electrochemical biosensor for glucose, DNA and protein using gold-polyaniline nanocomposites as a common matrix. *Sens. Actuators B* **2014**, *190*, 348-356.

[S4] Rahman, S. A.; Ariffin, N.; Yusof, N. A.; Abdullah, J.; Mohammad, F.; Zubir, Z. A.; Aziz, N. M. A. N. A. Thiolate-Capped CdSe/ZnS Core-Shell Quantum Dots for the Sensitive Detection of Glucose. *Sensors* **2017**, *7*, 1537.

[S5] Huang, Y.; Shi, Y.; Yang, H. Y.; Ai, Y. A novel single-layered MoS_2 nanosheet based microfluidic biosensor for ultrasensitive detection of DNA. *Nanoscale* **2015**, *7*, 2245-2249.

[S6] Park, J. W.; Lee, C.; Jang, J. High-performance field-effect transistor-type glucose biosensor based on nanohybrids of carboxylated polypyrrole nanotube wrapped graphene sheet transducer. *Sens. Actuators B* **2015**, *208*, 532-537.

[S7] Presnova, G.; Presnov, D.; Krupenin, V.; Grigorenko, V.; Trifonov, A.; Andreeva, I.; Ignatenko, O.; Egorov, A.; Rubtsova, M. Biosensor based on a silicon nanowire field-effect transistor functionalized by gold nanoparticles for the highly sensitive determination of prostate specific antigen. *Biosens. Bioelectron*. **2008**, *88*, 283-289.

[S8] Liu, Q.; Liu, Y.; Wu, F.; Cao, X.; Li, Z.; Alharbi , M.; Abbas, A. N. Highly Sensitive and Wearable In_2O_3 Nanoribbon Transistor Biosensors with Integrated On-Chip Gate for Glucose Monitoring in Body Fluids. *ACS Nano* **2018**, *12*, 1170-1178.

[S9] Sarkar, D.; Liu, W.; Xie, X.; Anselmo, A. C.; Mitragotri, S.; Banerjee, K. MoS_2 Field-Effect Transistor for Next-Generation Label-Free Biosensors. *ACS Nano* **2014**, *8*, 3992-4003.

[S10] Park, H. -Y.; Dugasani, S. R.; Kang, D. -H.; Jeon, J.; Jang, S. K.; Lee, S.; Roh, Y.; Park, S. H.; Park, J. -H. n- and p-Type Doping Phenomenon by Artificial DNA and M-DNA on Two-Dimensional Transition Metal Dichalcogenides. *ACS Nano* **2014**, *8*, 11603-11613.